THE JOURNAL OF BIOLOGICAL CHEMISTRY VOL. 287, NO. 21, pp. 17186–17197, May 18, 2012

ATP Synthesis-coupled and -uncoupled Acetate Production from Acetyl-CoA by Mitochondrial Acetate:Succinate CoA-transferase and Acetyl-CoA Thioesterase in *Trypanosoma*[*] [S]

Received for publication, February 22, 2012, and in revised form, March 30, 2012 Published, JBC Papers in Press, April 2, 2012, DOI 10.1074/jbc.M112.355404

Yoann Millerioux[‡1], Pauline Morand[‡1], Marc Biran[‡], Muriel Mazet[‡], Patrick Moreau[§], Marion Wargnies[‡], Charles Ebikeme[‡], Kamel Deramchia[‡], Lara Gales[¶‖], Jean-Charles Portais[¶‖**], Michael Boshart[‡‡], Jean-Michel Franconi[‡], and Frédéric Bringaud[‡2]**

*From the [‡]Centre de Résonance Magnétique des Systèmes Biologiques, UMR 5536, Université Bordeaux Segalen, CNRS, 146 Rue Léo Saignat, 33076 Bordeaux, France, the [§]Laboratoire de Biogenèse Membranaire, UMR 5200, Université Bordeaux Segalen, CNRS, 146 Rue Léo Saignat, 33076 Bordeaux, France, the [¶]Université de Toulouse, INSA, UPS, INP, LISBP, 135 Avenue de Rangueil, F-31077 Toulouse, France, the [‖]INRA, UMR792, Ingénierie des Systèmes Biologiques et des Procédés, F-31400 Toulouse, France, **CNRS, UMR5504, F-31400 Toulouse, France, [‡‡]Biozentrum, Genetik, Ludwig-Maximilians-Universität München, Grosshadernerstr, 2-4, D-82152 Martinsried, Germany*

Background: Mitochondrial acetate production is essential for viability of the procyclic trypanosomes and probably many other protists.
Results: We identified an acetyl-CoA thioesterase (ACH) contributing to acetate production from acetyl-CoA.
Conclusion: Acetate production by ASCT, but not by ACH, is involved in ATP production.
Significance: In trypanosomes and probably other protists, ASCT/SCoAS cycle-derived ATP production can substitute for oxidative phosphorylation.

Insect stage trypanosomes use an "acetate shuttle" to transfer mitochondrial acetyl-CoA to the cytosol for the essential fatty acid biosynthesis. The mitochondrial acetate sources are acetate:succinate CoA-transferase (ASCT) and an unknown enzymatic activity. We have identified a gene encoding acetyl-CoA thioesterase (ACH) activity, which is shown to be the second acetate source. First, RNAi-mediated repression of ASCT in the ACH null background abolishes acetate production from glucose, as opposed to both single ASCT and ACH mutants. Second, incorporation of radiolabeled glucose into fatty acids is also abolished in this ACH/ASCT double mutant. ASCT is involved in ATP production, whereas ACH is not, because the ASCT null mutant is ~1000 times more sensitive to oligomycin, a specific inhibitor of the mitochondrial F_0/F_1-ATP synthase, than wild-type cells or the ACH null mutant. This was confirmed by RNAi repression of the F_0/F_1-ATP synthase $F_1\beta$ subunit, which is lethal when performed in the ASCT null background but not in the wild-type cells or the ACH null background. We concluded that acetate is produced from both ASCT and ACH; however, only ASCT is responsible, together with the F_0/F_1-ATP synthase, for ATP production in the mitochondrion.

Many protists, including parasitic helminths, amoeba, diplomonads, trichomonads, and trypanosomatids, produce and excrete acetate as a major metabolic end product of their energy metabolism (1, 2). In all of these eukaryotic organisms, acetate production is considered to be coupled to ATP production. Acetate is mainly produced by two different reactions catalyzed by either a cytosolic acetyl-CoA synthetase (ADP-forming) or an organellar acetate:succinate CoA-transferase (ASCT).[3] Acetyl-CoA synthetase generates ATP by substrate level phosphorylation, whereas the involvement of ASCT in ATP production requires the succinyl-CoA synthase (SCoAS) activity (see supplemental Fig. S1). Indeed, it has been proposed that ASCT transfers the CoA group of acetyl-CoA to succinate to form succinyl-CoA, which is consequently converted back to succinate by SCoAS with a net production of one molecule of ATP per molecule of acetyl-CoA (3).

ASCT and SCoAS are located in the same subcellular compartment in all trypanosomatids, including *Trypanosoma brucei* (3), in all helminths analyzed so far, such as *Fasciola hepatica* and *Brugia malayi* (4, 5), *Nyctotherus ovalis* (6), *Trichomonas vaginalis* (7), *Neocallimastix* (8), *Blastocistis* sp. (9), and *Naegleria gruberi* (10). However, the ATP production by the proposed ASCT/SCoAS cycle has not been experimentally demonstrated so far in any of these organisms. To address this key question as a model, we use the procyclic form of *T. brucei*.

The procyclic form of *T. brucei* primarily converts glucose, the main carbon source consumed in rich medium, into succi-

* This work was supported by CNRS, the Université Bordeaux Segalen, the Conseil Régional d'Aquitaine, the Fondation pour la Recherche Médicale, Agence Nationale de la Recherche programs (Grants METABOTRYP of the ANR-MIME2007 call, SysTryp of the ANR-BioSys2007 call, and ACETOTRYP of the ANR-BLANC-2010 call), Prod'Innov, and Franco-Bavarian University Cooperation Center Grant BFHZ/CCUFB (to M. B. and F. B.).
[S] This article contains supplemental Figs. S1–S3.
[1] Both authors contributed equally to this work.
[2] To whom correspondence should be addressed. Tel.: 33-5-57-57-46-32; Fax: 33-5-57-57-45-56; E-mail: bringaud@rmsb.u-bordeaux2.fr.

[3] The abbreviations used are: ASCT, acetate:succinate CoA-transferase; ACH, acetyl-CoA thioesterase or acetyl-CoA hydrolase; ATPϵ, mitochondrial F_0/F_1-ATP synthase; EGFP, enhanced green fluorescent protein; ERETIC, electronic reference to access *in vivo* concentrations; hsp60, heat shock protein 60; SCoAS, succinyl-CoA synthetase; TCA, tricarboxylic acid.

nate and acetate (11, 12). Acetate is produced in the mitochondrion of the parasite, where the ASCT activity and protein are located (3, 13). We characterized the *ASCT* gene and showed that RNAi down-regulation of ASCT expression or *ASCT* gene deletion did not abolish acetate production from glucose, although its relative excretion was significantly reduced (13). This indicated at least one additional enzymatic activity contributing to acetate production. Interestingly, upon ablation of pyruvate dehydrogenase expression, the enzyme that converts pyruvate to acetyl-CoA, acetate is no longer produced from glucose (14). This implied that the alternative source of acetate was acetyl-CoA.

Here, we show that the *Tb927.3.4260* (see the TriTrypDB Web site) gene product, encoding a putative mitochondrial acetyl-CoA thioesterase (also called acetyl-CoA hydrolase (ACH)), is contributing to acetate production. RNAi-mediated repression of both ASCT and ACH proteins led to a complete cessation of glucose-derived acetate excretion. Whereas ACH is not involved in ATP production, the ASCT contribution to the mitochondrial ATP production can substitute for oxidative phosphorylation and *vice versa*.

EXPERIMENTAL PROCEDURES

Growth and Maintenance of Trypanosomes—The procyclic form of *T. brucei* EATRO1125.T7T (*TetR-HYG T7RNAPOL-NEO*) was cultured at 27 °C in SDM79 medium containing 10% (v/v) heat-inactivated fetal calf serum (FCS) and 25 μg/ml hemin (15).

Gene Knockout of ACH and ASCT—Replacement of ACH (Tb927.3.4260; see the TriTrypDB Web site) or ASCT (Tb11.02.0290) genes by the blasticidin and puromycin resistance markers via homologous recombination was performed with DNA fragments containing a resistance marker gene flanked by the ACH or ASCT UTR sequences, as performed before (16). Briefly, the pGEMt plasmid was used to clone an HpaI DNA fragment containing the blasticidin and puromycin resistance marker genes preceded by the ACH or ASCT 5′-UTR fragment (537 or 492 bp) and followed by the ACH or ASCT 3′-UTR fragment (521 or 485 bp). The ACH and ASCT knockouts were generated in the EATRO1125.T7T parental cell line, which constitutively expresses the T7 RNA polymerase gene and the tetracycline repressor under the control of a T7 RNA polymerase promoter for tetracycline-inducible expression (17). Transfection and selection of drug-resistant clones were performed as reported previously (18). Transfected cells, called Δ*ach* (*TetR-HYG T7RNAPOL-NEO* Δ*ach*::*BLA*/Δ*ach*::*PURO*) and Δ*asct* (*TetR-HYG T7RNAPOL-NEO* Δ*asct*::*BLA*/Δ*asct*::*PURO*), were selected in SDM79 medium containing hygromycin B (25 μg/ml), neomycin (10 μg/ml), blasticidin (10 μg/ml), and puromycin (1 μg/ml).

Inhibition of Gene Expression by RNAi—The inhibition by RNAi of gene expression in the procyclic form (19) was performed by expression of stem-loop "sense-antisense" RNA molecules of the targeted sequences (17) introduced in the pLew100 (kindly provided by E. Wirtz and G. Cross) (20) or pHD1336 (kindly provided by C. Clayton, ZMBH, Heidelberg, Germany) expression vectors, as described previously. These vectors contain the phleomycin and blasticidin resistance genes, respectively. Construction of pLew-ASCT-SAS and pLew-ATPϵ-F1β-SAS (ATPϵ-F1β, F1β subunit of the F_0/F_1-ATP synthase, Tb927.3.1380), used to produce the Δ*ach*/^{RNAi}ASCT, Δ*ach*/^{RNAi}ATPϵ-F1β, and Δ*asct*/^{RNAi}ATPϵ-F1β double mutants has been described before (13, 14). The ^{RNAi}ASCT and ^{RNAi}ATPϵ-F1β cell lines have been generated before (13, 14). The pHD-ACH-SAS construct targets a fragment (from position 76 to 576 bp) of the *ACH* gene. Briefly, a PCR-amplified 592-bp fragment, containing the antisense ACH sequence with restriction sites added to the primers, was inserted into the HindIII and BamHI restriction sites of the pLew100 plasmid. Then separate PCR-amplified fragments containing the sense ACH sequence was inserted upstream of the antisense sequence, using HindIII and XhoI restriction sites (XhoI was introduced at the 3′-extremity of the antisense PCR fragment). Finally, the "sense-antisense" HindIII/BamHI cassette was inserted in the HindIII/BamHI-digested pHD1336 vector. The resulting plasmid (pHD-ACH-SAS) contains a sense and antisense version of the targeted gene fragment, separated by a 50-bp fragment, under the control of the PARP polymerase promoter linked to a prokaryotic tetracycline operator.

The Δ*ach* and Δ*asct* null mutants and the EATRO1125.T7T parental cell line have been transformed with pLew100 constructs described above (pLew-ATPϵ-F1β-SAS). The RNAi-harboring single mutant cell lines were selected in SDM79 medium containing hygromycin B (25 μg/ml), neomycin (10 μg/ml), and phleomycin (5 μg/ml). For transfection of the Δ*ach* and Δ*asct* cell line, blasticidin (10 μg/ml) and puromycin (1 μg/ml) were also included in the medium. The EATRO1125.T7T and ^{RNAi}ASCT cell lines were transfected with the pHD-ACH-SAS construct, and blasticidin (10 μg/ml) was used to select recombinant cell lines in addition to hygromycin B/neomycin and hygromycin B/neomycin/phleomycin, respectively. Aliquots of each were frozen in liquid nitrogen to provide stocks of each line that had not been cultivated long term in medium.

Inhibition of Mitochondrial F_0/F_1-ATP Synthase by Oligomycin—*T. brucei* EATRO1125.T7T, Δ*ach*, and Δ*asct* cell lines were cultivated at 27 °C in SDM79. This assay was performed in 96-well microtiter plates with 100 μl of cell suspension (5×10^5/ml)/well in the presence of decreasing quantities of oligomycin (from 20 μg/ml to 0.012 pg/ml). The concentration of oligomycin required to kill all of the cells (lethal dose 100; LD_{100}) was determined optically at 24 h and every 48 h during 13 days after drug addition.

Immune Sera Production and Western Blot Analyses—For the production of ACH antibodies, a recombinant fragment corresponding to the full-length *ACH* gene preceded by an N-terminal histidine tag (6 histidine codons) was expressed in the *Escherichia coli* BL21(DE3), using the pET3a expression vector (Novagen). Cells were harvested by centrifugation, and recombinant proteins contained in the insoluble fraction were purified by nickel chelation chromatography in the presence of 6 M urea (Novagen), according to the manufacturer's instructions. Antisera were raised in rabbits by five injections at 15-day intervals of 100 μg of ACH-His recombinant nickel-purified proteins, emulsified with complete (first injection) or incom-

plete Freund's adjuvant (Proteogenix S.A.). Because the immune sera diluted up to 20 times did not detect the native ACH in trypanosome extracts by Western blotting, we purified the anti-ACH antibodies against a recombinant peptide corresponding to an N-terminal part of the *ACH* gene. A PCR fragment corresponding to positions 135–651 bp (amino acids 45–217) of the *ACH* gene was cloned in the NdeI and BamHI restriction sites of the pET28a expression vector (Novagen). Expression and purification by nickel chelation of the histidine-tagged ACHNter peptide was performed as described for the full-length histidine-tagged recombinant ACH. Approximately 1 mg of the purified His-tagged ACHNter peptide was blotted on a PVDF membrane (2 cm^2). After blocking with 5% dry milk in phosphate-buffered saline (PBS) for 1 h at room temperature, the membrane was incubated overnight at 4 °C with the immune serum (10 ml). The antibodies were eluted by a 10-min incubation in 1 ml of 100 mM glycine, pH 2.5, and the eluate was neutralized by the addition of 50 μl of 100 mM Tris, pH 8.

Total protein extracts of procyclic form *T. brucei* (5×10^6 cells) were separated by SDS-PAGE (10%) and immunoblotted on Immobilon-P filters (Millipore) (21). Immunodetection was performed as described (21, 22) using as primary antibodies the rabbit antisera against ACH diluted 1:500, ASCT diluted 1:1,000 (13), and the F1 moiety of the mitochondrial F_0/F_1-ATP synthase isolated from *Crithidia fasciculata* diluted 1:1,000 (23) (gift from D. Speijer, Amsterdam, Netherlands) or the mouse antiserum against heat shock protein 60 (hsp60) diluted 1:10,000 (24). Goat anti-rabbit or anti-mouse Ig/peroxidase (1:10,000 dilution) was used as secondary antibody, and revelation was performed using the SuperSignal® West Pico chemiluminescent substrate as described by the manufacturer (Thermo Scientific). Images were acquired and analyzed with a KODAK Image Station 4000 MM, and quantitative analyses were performed with the KODAK MI application.

Overexpression and Purification of ACH in Procyclic Cells—The pHD1336 expression vector was used to produce the full-length recombinant ACH protein containing (pHD-ACH$^+$his) or not (pHD-ACH$^+$) a C-terminal histidine tag (6 histidine codons), by inserting a 1,122- or 1,140-bp PCR fragment, respectively, in the HindIII and BamHI restriction sites of the pHD11336 plasmid. The pHD-ACH$^+$ and pHD-ACH$^+$his plasmids were introduced in the EATRO1125.T7T and ^{RNAi}ASCT cell lines (*TetR-HYG T7RNAPOL-NEO* ^{RNAi}*ASCT-BLE*). Expression of the ACH recombinant protein together (^{RNAi}ASCT/ACH$^+$.i and ^{RNAi}ASCT/ACH$^+$his.i) or not (ACH$^+$.i and ACH$^+$his.i) with RNAi inhibition of the *ASCT* gene expression was tetracycline-induced 48 h at 27 °C.

Enzyme Assays—Sonicated (5 s at 4 °C) crude extracts of trypanosomes resuspended in cold hypotonic buffer (10 mM potassium phosphate, pH 7.8) or trypanosome fractions containing ACH-His recombinant proteins purified by nickel chelation chromatography were tested for ACH (EC 3.1.2.1) and glycerol-3-phosphate dehydrogenase (EC 1.1.1.8) activities (25). ACH activity was measured spectrophotometrically as production of CoA by a 4,4′-dithiodipyridine (Aldrithiol) assay, modified by P. P. Van Veldhoven from protocols described previously (26, 27). Aldrithiol reacts with free CoASH, and formation of one of the reaction products, 4-thiopyridine, is followed at 324 nm (ϵ_{324} = 19,800/M/cm). The reaction mixture contained 50 mM HEPES (pH 7.4), 0.25 mM EDTA (pH 7.4), 0.2 mM aldrithiol, 0.05% (w/v) Thesit, and 5×10^6 cells resuspended in cold hypotonic buffer, in a final volume of 0.5 ml. Acetyl-CoA was added as a substrate at 0.1 mM. To test the ACH substrate specificity, 0.1 mM acetyl-CoA was replaced by the same concentration of malonyl-CoA (C3), crotonoyl-CoA (C4), acetoacetyl-CoA (C4), hydroxybutyryl-CoA (C4), butyryl-CoA (C4), hexanoyl-CoA (C6), octanoyl-CoA (C8), decanoyl-CoA (C10), lauroyl-CoA (C12), myristoyl-CoA (C14), palmitoyl-CoA (C16), palmitoleoyl-CoA (C16:1), stearoyl-CoA (C18), oleoyl-CoA (C18:1), and arachidonoyl-CoA (C20).

Construction of Enhanced Green Fluorescent Protein (EGFP)-tagged ACH in Trypanosomes and Immunofluorescence Analyses—Recombinant fragments corresponding to the N-terminal extremity of the *ACH* gene, with or without the N-terminal mitochondrial signal (33 residues), followed by the EGFP, were expressed in the procyclic form using the pLew100 vector. PCR fragments corresponding to the first 164 amino acids of ACH (pLew-ACH-1/164.EGFP) and the same region deleted for the N-terminal 33 residues (pLew-ACH-34/164.EGFP) were inserted between the XhoI (or HindIII) and XbaI restriction sites of the pLew100-EGFP1 plasmid described previously (28).

To stain mitochondria of the wild type and ACH$^+$.i procyclic cell lines, 200 nM MitoTracker® Red CMXRos (Invitrogen) were added to the culture, followed by a 20-min incubation and washes in PBS. For immunofluorescence analyses, wild type, ACH$^+$.i, ACH-1/164.EGFP.i, and ACH-34/164.EGFP.i cells were fixed with 4% formaldehyde in PBS, permeabilized with 1% Triton X-100, and spread on poly-L-lysine-coated slides. The slides were then incubated for 45 min in PBS containing 5% BSA, followed by incubation in PBS with 2% BSA and the primary antiserum, 1:200 diluted rabbit polyclonal anti-ACH or 1:100 diluted rabbit anti-ASCT (13). After washing with PBS, the slides were incubated with 2 μg/ml Alexa 594 anti-rabbit IgG conjugate or Alexa Fluor 488 anti-rabbit IgG conjugate (Molecular Probes). Slides were then washed and mounted in the SlowFade® antifade reagent (Invitrogen). Cells were visualized with a Leica DM5500B microscope, and images were captured by an ORCA®-R^2 camera (Hamamatsu) and Leica MM AF Imaging System software (MetaMorph®).

Analysis of Excreted End Products from Glucose Metabolism—1×10^8 *T. brucei* procyclic cells were collected by centrifugation at 1,400 × *g* for 10 min, washed once with PBS, and incubated in 5 ml of PBS supplemented with 2 g/liter $NaHCO_3$ (pH 7.4). Cells were maintained for 6 h at 27 °C in incubation buffer containing 20 μmol of D-glucose (4 mM). The integrity of the cells during the incubation was checked by microscopic observation. The supernatant was collected, and 50 μl of maleate solution in D_2O (20 mM) was added as an internal reference. ^{1}H-NMR spectra were performed at 125.77 MHz on a Bruker DPX500 spectrometer equipped with a 5-mm broadband probe head. Acquisition conditions were as follows: 90° flip angle, 5,000 Hz spectral width, 32 K memory size, and 9.3 s total recycle time. The relaxation delay was 6 s for a nearly complete longitudinal relaxation. Measurements were recorded at 25 °C with an electronic reference to access *in vivo* concentrations (ERETIC) method, which provides an electronically synthe-

sized reference signal on the proton spectrum (29). This reference was placed at 0.2 ppm to avoid superposition on sample resonances. Measurements were performed with 256 scans for a total time close to 40 min. Before each experiment, the phase of the ERETIC peak was precisely adjusted. Resonances of obtained spectra (succinate at 3.35 ppm, pyruvate at 3.32 ppm, acetate at 1.87 ppm, alanine at 1.43 ppm, and lactate at 1.28 ppm) were integrated, and results were expressed relative to ERETIC peak integration.

Lipid Labeling from [U-^{14}C]Glucose—10^8 cells in the late exponential phase were incubated for 16 h in 5 ml of SDM79 medium without L-threonine, containing 3 mM D-glucose and 25 μCi of D-[U-^{14}C]glucose (300 mCi/mmol; PerkinElmer SAS, Courtaboeuf, France) or containing 3 mM D-glucose, 1 mM acetate, and 10 μCi of [1-^{14}C]acetate (55.3 mCi/mmol; PerkinElmer SAS). Cells were checked microscopically for viability during the incubation. Subsequently, lipids were extracted by chloroform/methanol (2:1, v/v) for 30 min at room temperature and then washed three times with 0.9% NaCl. The solvent was evaporated, and lipids were dissolved in an appropriate volume of chloroform/methanol (1:1, v/v). Polar lipids were analyzed by loading total lipids onto HPTLC plates (60F254, Merck), which were developed in methyl acetate, *n*-propanol, chloroform, methanol, 0.25% aqueous KCl (25:25:25:10:9; v/v/v/v/v) (30). To analyze neutral lipids, total lipids were loaded onto HPTLC plates developed in hexane/ethylether/acetic acid (90:15:2, v/v/v) and diacylglycerols (R_F = 0.08), free fatty acids (R_F = 0.29), and triacylglycerols (R_F = 0.50) were separated. Lipids were identified by co-migration with known standards. Lipid radioactivity was determined with a Storm 860 molecular imager from GE Healthcare.

Determination of Intracellular ATP Concentrations—The intracellular ATP concentrations were determined on established procyclic cells in mid-log growth phase, when applicable. Cell pellets (1–2 $\times$ 10^8 procyclic cells) were washed in cold PBS and frozen in liquid nitrogen. Lysis and deproteinization of the cellular pellets involved homogenization in 500 μl of cold perchloric acid (0.9 M) and neutralization (pH 6.5) by the addition of KOH/MOPS (2 M/0.5 M). Then ATP concentrations were determined with the firefly luciferase bioluminescence assay (ATPlite 1step Luminscent Assay, PerkinElmer SAS) (31).

RESULTS

Down-regulation of ASCT Expression in ACH Null Background Is Lethal for Procyclic Trypanosomes—We previously showed that procyclic trypanosomes produced acetate from acetyl-CoA by mitochondrial ASCT and an by unknown distinct activity (13). We screened the *T. brucei* genome databases (TriTrypDB and GeneDB) for homologues of all known enzymes producing acetate from acetyl-CoA. In addition to the previously characterized *ASCT* and acetyl-CoA synthetase (AMP-forming) genes (13, 32), we identified a single gene candidate containing the acyl-CoA thioesterase domain (COG1607; GeneDB) named acetyl-CoA thioesterase or ACH (Tb927.3.4260). ACH orthologs are present in the genome of all trypanosomatids sequenced so far, except *Trypanosoma cruzi* (TriTrypDB). ACH expression was down-regulated by RNAi in EATRO1125.T7T procyclic trypanosomes and derived ^{RNAi}ASCT cell lines to generate the ^{RNAi}ACH single and ^{RNAi}ASCT/^{RNAi}ACH double mutants, respectively. Upon RNAi induction by tetracycline addition, the ^{RNAi}ASCT/^{RNAi}ACH double mutant (^{RNAi}ASCT/^{RNAi}ACH.i) ceased growth, whereas the ^{RNAi}ACH.i and ^{RNAi}ASCT.i single mutants were not compromised (data not shown). However, the ^{RNAi}ASCT/^{RNAi}ACH cell line was not amenable to further analyses because of the rapid phenotypic reversion due to ASCT and/or ACH re-expression (data not shown).

As an alternative, we generated an ACH knock-out mutant (Δ*ach*::BLA/Δ*ach*::PURO, abbreviated as Δ*ach*) by replacing both *ACH* alleles by selectable markers in the procyclic EATRO1125.T7T background. Deletion of both *ACH* alleles in the selected Δ*ach* cell line was tested by PCR (Fig. 1*A*, *inset*) and Western blotting using immunopurified anti-ACH antibodies raised against the recombinant histidine-tagged *T. brucei* ACH (see Fig. 4*A*); the 44-kDa protein detected in the wild type procyclic cells, which is compatible with the ACH calculated size (41.3 kDa), is not detectable in the Δ*ach* cell line. As expected from growth of the ^{RNAi}ACH.i mutant, the Δ*ach* mutant showed no growth phenotype (Fig. 1*A*). For RNAi knockdown of *ASCT* in the Δ*ach* background, the pLew100-ASCT-SAS construct was introduced. The tetracycline-induced Δ*ach*/^{RNAi}ASCT cell line (Δ*ach*/^{RNAi}ASCT.i) showed a strong growth phenotype and complete growth arrest after 2 weeks of induction (Fig. 1*B*). In the single ^{RNAi}ASCT mutant, only a slight growth phenotype was observed upon tetracycline induction (Fig. 1*C*). These results establish that ASCT and ACH share a common function and act redundantly.

Acetate Production Is Abolished in Δach/^{RNAi}ASCT.i Double Mutant—Proton ^{1}H-NMR spectroscopy was used to detect and quantify the metabolic end products excreted from glucose metabolism. The parasites were incubated in PBS/$NaHCO_3$ medium containing 4 mM D-glucose as the only carbon source, and the incubation medium was analyzed by ^{1}H-NMR spectroscopy. The parental EATRO1125.T7T procyclic cells mainly excrete acetate and succinate (~80 and 19% of the excreted molecules, respectively) and traces of pyruvate under those conditions (Table 1 and Fig. 2). As observed previously (13), the rate of acetate excretion is significantly reduced in the tetracycline-induced ^{RNAi}ASCT.i mutant compared with uninduced cells (980 *versus* 1440 nmol/h/mg of protein, respectively), confirming that ASCT is contributing to acetate production. The rate of pyruvate excretion is ~9.5-fold increased in the mutant compared with the parental cells, probably as a consequence of product inhibition of pyruvate dehydrogenase by accumulating acetyl-CoA in the ^{RNAi}ASCT.i mutant (Table 1). Similarly, alanine production in the induced cell line may result from accumulation of pyruvate, which is the substrate of the alanine-producing enzyme alanine aminotransferase (33). It is also noteworthy that the rate of succinate production increased upon tetracycline induction (713 *versus* 231 nmol/h/mg of protein), suggestive of a metabolic flux redistribution at the phosphoenolpyruvate bifurcation (see supplemental Fig. S1). In the induced Δ*ach*/^{RNAi}ASCT.i line, the rate of acetate production is almost completely abolished, indicating that ASCT and ACH together fully account for mitochondrial acetate production (Table 1 and Fig. 2). Succinate and pyruvate become the major

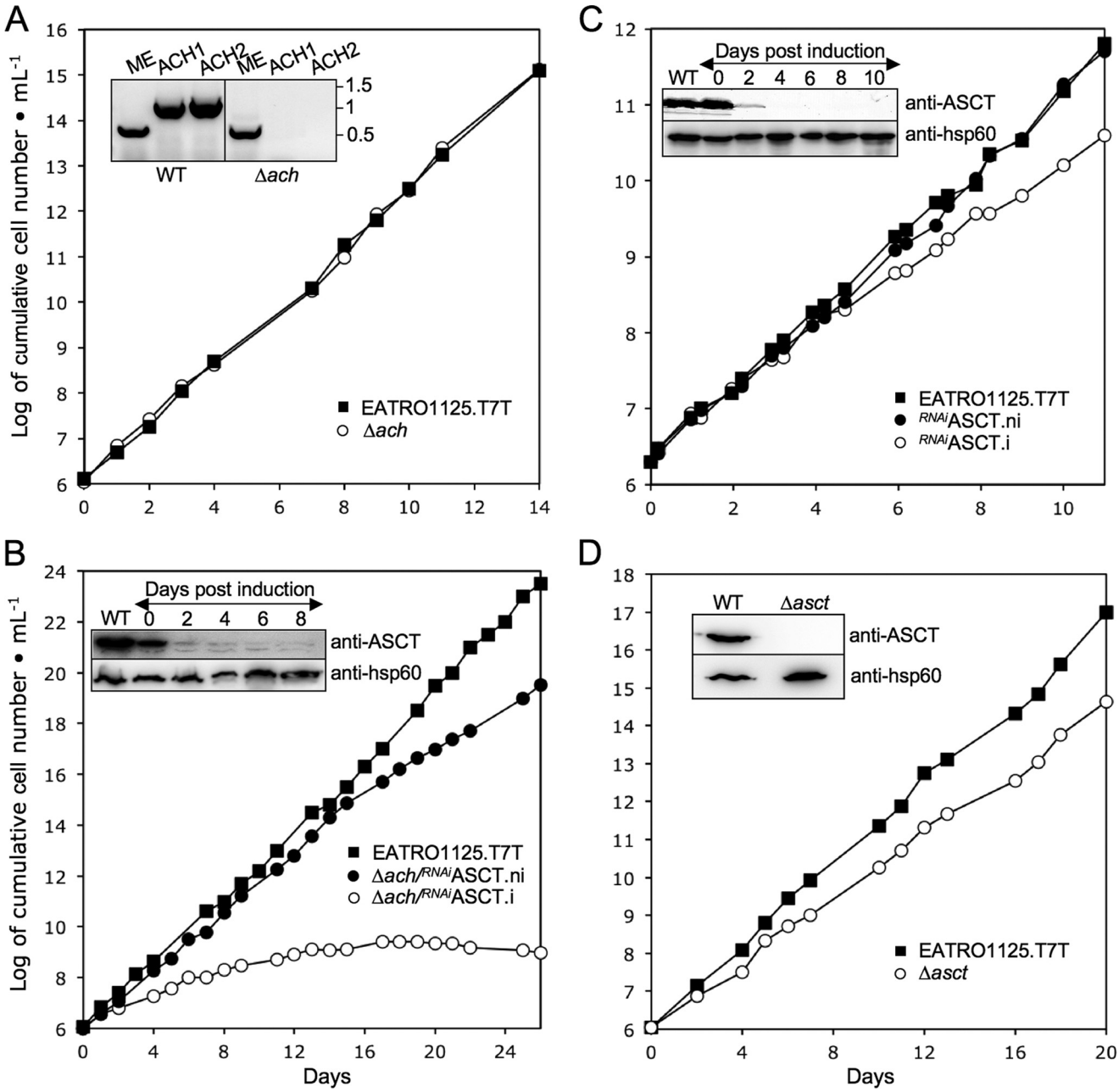

FIGURE 1. **Analysis of ASCT and ACH mutant cell lines.** Growth curves of the Δ*ach* (*A*) and Δ*asct* (*D*) null mutants and the Δ*ach*/^{RNAi}ASCT (*B*) and ^{RNAi}ASCT (*C*) cell lines incubated in the presence (.i; ○) or in the absence (.ni; ●) of tetracycline. Cells were maintained in the exponential growth phase (between 10^6 and 10^7 cells/ml) by dilution, and cumulative cell numbers are calculated. The *insets* show Western blot controls of ASCT expression in EATRO1125.T7T (WT) and Δ*asct* (*D*), Δ*ach*/^{RNAi}ASCT (*B*), and ^{RNAi}ASCT (*C*). Induction refers to tetracycline addition. The *inset* in *A* shows the locus PCR on genomic DNA isolated from the parental EATRO1125.T7T (WT) and Δ*ach*. Primers specific for the cytosolic malic enzyme (*ME*) (control) or *ACH* locus (ACH1 and ACH2) were used (see "Experimental Procedures").

end products excreted by the Δ*ach*/^{RNAi}ASCT.i double mutant (~2.4- and 46-fold increased compared with the parental cell line) (Table 1). The residual acetate production (~13-fold reduced compared with the parental cell line) is probably due to the low expression of ASCT, which is still detectable 8 days after induction of RNAi (Fig. 1*B*). Interestingly, no significant differences were observed between the parental and Δ*ach* cells, suggesting that the ASCT activity is alone sufficient to maintain the normal rate of acetate production (Table 1 and Fig. 2).

ACH Is Mitochondrial Protein—Immunofluorescence analyses with the immunopurified anti-ACH antibodies were not sufficiently sensitive to detect the native ACH protein in procyclic trypanosomes. To determine the subcellular localization, the *ACH* ORF was inducibly overexpressed in EATRO1125.T7T procyclic cells using the pHD1336 vector. ACH$^+$ cells overexpress (~50-fold) a 44-kDa protein recognized by the anti-ACH antibody (see supplemental Fig. S2*A*). Immunofluorescence analyses of the ACH$^+$ cell line using the anti-ACH immune serum revealed a "mitochondrion-like" reticulate pattern matching the mitochondrion-specific dye Mitotracker® Red CMXRos (Invitrogen) (Fig. 3*A*). The same mitochondrial pattern was also observed with the first 164 amino acids of ACH

TABLE 1

Excreted end products of D-glucose metabolism by procyclic *T. brucei* cell lines

The extracellular PBS medium of trypanosome cell lines incubated in the presence of 4 mM glucose was analyzed by ^{1}H-NMR spectrometry to detect and quantify excreted end products.

Cell line[a]	n[b]	Excreted molecules[c]					
		Acetate	Succinate	Pyruvate	Alanine	Lactate	Total
		nmol/h/mg of protein (% of excreted molecules)					
EATRO1125.T7T	3	1,343 ± 113 (79.7)	344 ± 45 (19.1)	21 ± 24 (1.2)	ND[d]	ND	1,708 ± 181 (100)
ASCT.ni	4	1,440 ± 217 (81.1)	231 ± 53 (13.7)	36 ± 28 (2.2)	ND	ND	1,707 ± 173 (100)
ASCT.i	4	980 ± 149 (48.7)	713 ± 164 (35.2)	199 ± 37 (10.0)	121 ± 18 (6.1)	ND	2,013 ± 278 (100)
Δ*ach*	3	1,498 ± 90 (82.1)	309 ± 28 (16.9)	19 ± 20 (1.0)	ND	ND	1,826 ± 138 (100)
Δ*ach*/ASCT.ni	4	1,151 ± 95 (64.1)	549 ± 68 (30.5)	82 ± 12 (4.5)	14 ± 29 (0.9)	ND	1,796 ± 133 (100)
Δ*ach*/ASCT.i	4	105 ± 31 (6.1)	829 ± 185 (47.0)	686 ± 54 (39.5)	103 ± 60 (6.0)	24 ± 27 (1.5)	1,747 ± 173 (100)
ACH$^+$.ni	4	1,511 ± 78 (83.4)	262 ± 91 (14.3)	43 ± 27 (2.3)	ND	ND	1,816 ± 114 (100)
ACH$^+$.i	4	1,483 ± 84 (82.2)	242 ± 27 (13.6)	57 ± 22 (3.2)	ND	ND	1,782 ± 115 (100)
ASCT/ACH$^+$.ni	3	1,384 ± 131 (82.8)	254 ± 28 (15.2)	28 ± 16 (1.7)	6 ± 10 (0.4)	ND	1,672 ± 133 (100)
ASCT/ACH$^+$.i	3	1,366 ± 71 (84.8)	216 ± 29 (13.3)	34 ± 17 (2.0)	ND	ND	1,616 ± 102 (100)

[a] .i, RNAi cell lines tetracycline-induced during 6–10 days, depending on the cell line and the experiments; .ni, non-induced RNAi cell lines.
[b] Number of experiments.
[c] Mean ± S.D. of three or four experiments (nmol/h/mg of protein) and the percentage of each excreted molecule (values in parentheses) are presented.
[d] Not detectable.

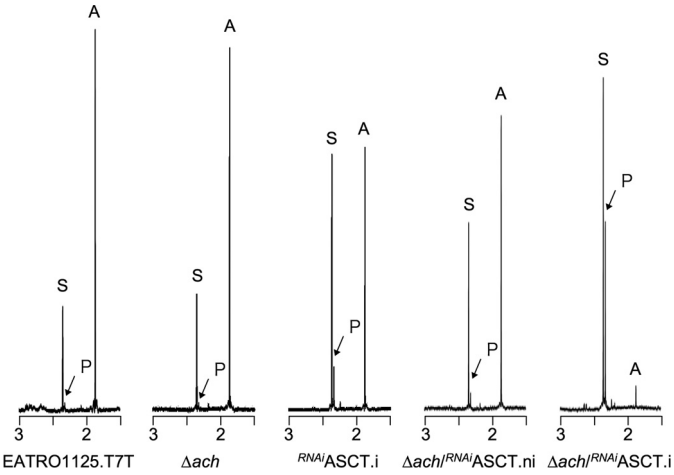

FIGURE 2. **Proton ^{1}H-NMR spectra of metabolic end products excreted by procyclic cell lines incubated with D-glucose.** The parental EATRO1125.T7T, Δ*ach*, tetracycline-induced (*.i*), or non-induced (*.ni*) ^{RNAi}ASCT and Δ*ach*/^{RNAi}ASCT cell lines were incubated with 4 mM D-glucose in PBS/$NaHCO_3$ buffer for 6 h. Each spectrum corresponds to one representative experiment from a set of at least three. The spectrum detail ranging from 1.5 to 3 ppm is shown. The resonances indicated are acetate (*A*), pyruvate (*P*), and succinate (*S*).

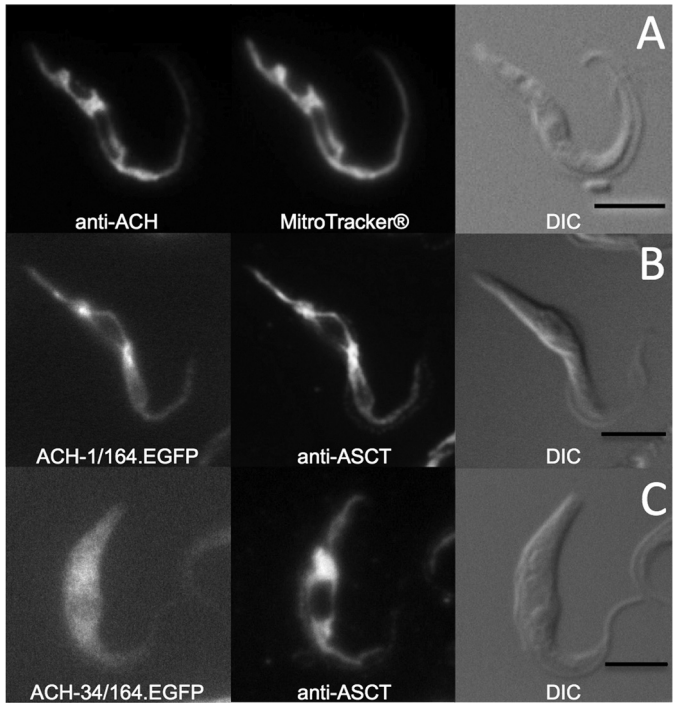

FIGURE 3. **Immunolocalization of ACH.** ACH$^+$ cell line (*A*) was stained with rabbit anti-ACH (Alexa 488 channel) and MitoTracker®. ACH-1/164.EGFP (*B*) and ACH-34/164.EGFP (*C*) cell lines were stained with rabbit anti-ASCT (Alexa 594 channel). Differential interference contrast (*DIC*) of cells is shown to the *right* of each *panel*. *Scale bar*, 5 μm.

fused to EGFP (Fig. 3*B*). Deletion of the first 33 residues in the previous construct gave a homogenous diffuse fluorescence pattern characteristic for a cytoplasmic localization (Fig. 3*C*). Thus, the N-terminal MLRRCFTPSHLIPFLCGGCLSSRRQLVVGNSKN peptide contains a functional mitochondrial targeting sequence as predicted by Mitoprot (available on the World Wide Web; 0.97 probability).

The ACH Gene Encodes Acetyl-CoA Thioesterase—Acetyl-CoA thioesterase activity was barely detectable in EATRO1125.T7T crude extracts (<5 milliunits/mg of proteins; see supplemental Fig. S3*A*). In the tetracycline-induced ACH$^+$his cell line, 29.7 ± 0.7 milliunits/mg of proteins were measured, in agreement with the ~50-fold increase of the ACH protein compared with wild type cells (Fig. 4*A* and supplemental Fig. S3*B*), indicating that ACH is a bona fide acetyl-CoA thioesterase. To determine the specific activity of the protein, the histidine-tagged protein overexpressed in the ACH$^+$his.i cell line was purified by nitrilotriacetic acid affinity chromatography, as shown in Fig. 4*B* (see supplemental Fig. S3*C*). The purification of a single 44-kDa protein detectable by Coomassie staining and recognized by the anti-ACH immune serum resulted in a ~130-fold increase of the ACH specific activity. This corresponded to a yield of ~200 μg of recombinant ACH purified from 3×10^9 ACH$^+$his cells. The maximum catalytic activity of the recombinant histidine-tagged ACH is 3.9 ± 0.33 units/mg of protein, which corresponds to a calculated k_{cat} for hydrolysis of acetyl-CoA of 2.7 s^{-1}.

Substrate specificity was determined by testing the ability of the ACH$^+$his-purified protein to hydrolyze short- and long-chain fatty acids ranging from C2 to C20 (Table 2). The highest thioesterase activity was observed with acetyl-CoA (C2) and C4 fatty acyl-CoA (butyryl-CoA, hydroxybutyryl-CoA, and acetoacetyl-CoA). ACH$^+$his shows a lower thioesterase activity with

crotonyl-CoA (C4) and hexanoyl-CoA (C6) and no significant activity with malonyl-CoA (C3) and other acyl-CoA (from C8 to C20).

Interestingly, we did not observe any decrease of the acetyl-CoA thioesterase activity by the addition of 50 mM succinate (data not shown). Because the enzymatic assay is based on the measurement of released CoASH, this indicates that ACH has no CoA-transferase activity to succinate, in contrast to ASCT (3).

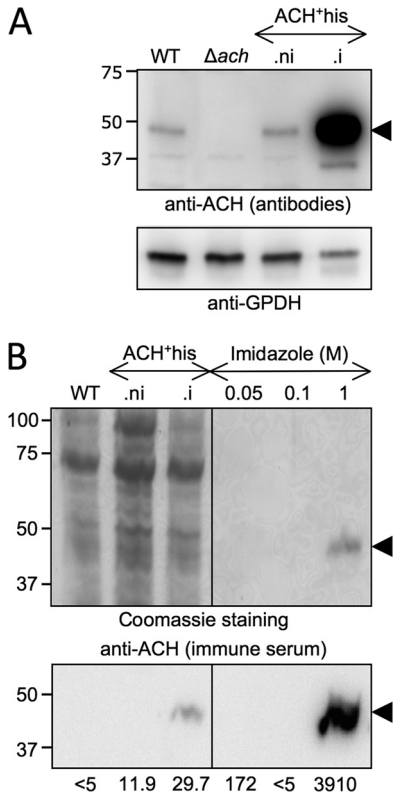

FIGURE 4. **Overexpression and purification of ACH.** Lysates of *T. brucei* EATRO1125.T7T procyclic form (*WT*), Δ*ach*, non-induced (*.ni*), and tetracycline-induced (*.i*) ACH$^+$his cell lines were analyzed by Western blotting with the immunopurified anti-ACH antibodies and the anti-glycerol-3-phosphate dehydrogenase (*GPDH*) immune serum (*A*). Samples contained 5×10^6 cells, except for ACH$^+$his.i (1.5×10^6 cells). ACH overexpression in ACH$^+$his.i was quantified using the KODAK Image Station 4000 MM. *B*, purification by nickel chelation of the ACH$^+$his. *Top panel*, Coomassie staining of lysates (5×10^6 cells) of wild type procyclic cell, non-induced, and tetracycline-induced ACH$^+$his cell lines and elution fractions sequentially obtained by nickel chelation with different imidazole concentrations. For each elution condition (0.05, 0.1, and 1 M), only the first of the three collected fractions is shown. The *bottom panel* shows the corresponding Western blot with the anti-ACH immune serum. The specific acetyl-CoA thioesterase activity (milliunits/mg of protein) measured for each sample is indicated *below* the Western blot. The positions of the molecular weight markers are indicated in kDa on the *left* of each *panel*.

ACH Overexpression Rescues Metabolic Phenotype of ASCT Deficiency—The decrease of acetate production (1.6-fold) and increase of succinate and pyruvate production (2.8- and 5.1-fold, respectively) in induced ^{RNAi}ASCT.i cells (Table 1) shows that ASCT cannot alone account for the wild type acetate production level. To confirm the role of ACH in acetate production, we rescued maximal acetate excretion by overexpressing ACH in the ^{RNAi}ASCT mutant (^{RNAi}ASCT/ACH$^+$ cell line). The simultaneous down-regulation of ASCT expression and ACH overexpression in the ^{RNAi}ASCT/ACH$^+$.i cell line was confirmed by Western blot analysis (supplemental Fig. S2*B*). The amounts of acetate, succinate, and pyruvate excreted from glucose metabolism remained unchanged upon double induction, indicating that ACH overexpression compensates for loss of ASCT. Interestingly, the significant overexpression of ACH (~50-fold) in the wild type background (ACH$^+$ cell line), does not increase the rate of acetate production (Table 1), suggesting that another step of the glucose catabolism is rate-limiting.

Fatty Acid Biosynthesis from Glucose Is Abolished in Δach/^{RNAi}ASCT Mutant—We previously demonstrated that acetyl-CoA used to feed fatty acid biosynthesis is produced from acetate by the essential cytosolic enzyme acetyl-CoA synthetase (AMP-forming), defining the acetate shuttle as a replacement for the more common citrate shuttle (32) (supplemental Fig. S1). Because glucose-derived acetate is produced by ASCT and ACH, we compared *de novo* fatty acid biosynthesis in the tetracycline-induced or non-induced Δ*ach*/^{RNAi}ASCT double mutant and the parental cell line incubated in growth medium containing D-[U-^{14}C]glucose. ^{14}C label incorporation in free fatty acids as well as in lipids containing fatty acids, *i.e.* phospholipids (phosphatidylcholine, phosphatidylinositol, and phosphatidylethanolamine), diacylglycerol, and triacylglycerol, is presented in Fig. 5. After 14 days of tetracycline induction, ^{14}C label incorporation is almost completely abolished in free fatty acids (15-fold reduction) and glycerolipids (from 7- to 48-fold reduction in phosphatidylethandamine and triacylglycerol, respectively). Conversely, we did not observe any decrease of ^{14}C label incorporation into the different lipids when cells were incubated in the same medium containing [1-^{14}C]acetate, which bypasses the acetate production by ASCT and ACH. We conclude that conversion of acetyl-CoA into acetate by ASCT or ACH is essential for incorporation of glucose carbon into fatty acids.

ATP Production in ASCT/SCoAS Cycle—The mitochondrial F_0/F_1-ATP synthase (ATPϵ) produces ATP as the last step in oxidative phosphorylation but is not essential for growth of the EATRO1125 procyclic cell line in glucose-rich medium (14, 34) (see Fig. 6*B*). This implies that ATP production by substrate level phosphorylation in the cytosol (phosphoglycerate kinase

TABLE 2

Substrate specificity of the *T. brucei* ACH

ACH activities (milliunits/mg of purified ACH-his protein) were determined on the ACH-His recombinant protein purified by nickel chelation chromatography, using as substrates 0.1 mM acyl-CoA molecules ranging from 2 to 20 carbons (C2 to C20).

	Acyl-CoA (0.1 mM)							
	Acetyl-CoA (C2)	Malonyl-CoA (C3)	Crotonoyl-CoA (C4)	Hydroxybutyryl-CoA (C4)	Acetoacetyl-CoA (C4)	Butyryl-CoA (C4)	Hexanoyl CoA (C6)	C8 to C20
Specific activity (milliunits/mg of protein)	3,910 ± 329	<60	851 ± 198	1,893 ± 791	3,605 ± 312	7,300 ± 194	359.2 ± 7.6	<60

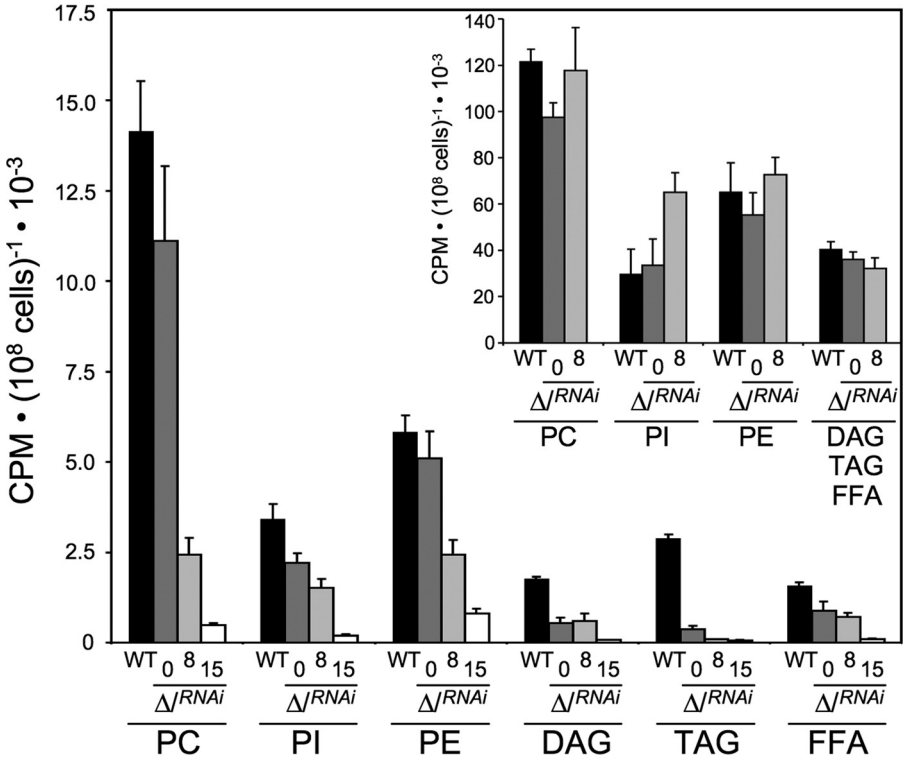

FIGURE 5. **D-[U-^{14}C]-glucose and [1-^{14}C]-acetate incorporation into lipids of the EATRO1125.T7T and Δ*ach*/^{RNAi}ASCT cell lines.** ^{14}C-labeled phospholipids (phosphatidylcholine (*PC*), phosphatidylinositol (*PI*), and phosphatidylethanolamine (*PE*)) and ^{14}C-labeled neutral lipids (diacylglycerol (*DAG*), triacylglycerol (*TAG*), and free fatty acids (*FFA*)) were separated by HPTLC and analyzed as described under "Experimental Procedures." Cells were incubated for 16 h in SDM79 containing D-[U-^{14}C]glucose or [1-^{14}C]acetate (*inset histogram*) prior to lipid extraction. *Black columns* correspond to the EATRO1125.T7T parental cell line (*column WT*), whereas *dark gray*, *light gray* and *white columns* correspond to the non-induced (*column 0*), tetracycline-induced for 8 days (*column 8*), and tetracycline-induced for 15 days (*column 15*) Δ*ach*/^{RNAi}ASCT cells, respectively. Shown is the mean ± S.D. (*error bars*) of three independent experiments.

and pyruvate kinase) and/or in the mitochondrion (SCoAS) can compensate for the chemical inhibition or RNAi-mediated down-regulation of ATPϵ. To determine whether the postulated ASCT/SCoAS cycle becomes essential for ATP production in the absence of oxidative phosphorylation, the EATRO1125.T7T, Δ*ach* and Δ*asct* cell lines were compared for their sensitivity to oligomycin, a specific inhibitor of ATPϵ. We observed that the Δ*asct* cell line is ~1,000 times more sensitive to the inhibitor than the EATRO1125.T7T cell line, whereas the Δ*ach* line is as sensitive as parental cells (Fig. 6*A*). This indicates that ASCT, but not ACH, becomes essential when ATPϵ is inhibited. To confirm these data, expression of ATPϵ F1β subunit was down-regulated by RNAi in the wild type (^{RNAi}ATPϵ-F1β), Δ*ach* (Δ*ach*/^{RNAi}ATPϵ-F1β), and Δ*asct* (Δ*asct*/^{RNAi}ATPϵ-F1β) backgrounds. No significant growth phenotype was observed for the ^{RNAi}ATPϵ-F1β single and the Δ*ach*/^{RNAi}ATPϵ-F1β double mutants (Fig. 6, *B* and *C*), whereas the ATPϵ-F1β is repressed below detectability on Western blots upon tetracycline induction. In contrast, the Δ*asct*/^{RNAi}ATPϵ-F1β double mutant is lethal upon tetracycline induction (Fig. 6*D*).

The intracellular ATP concentration was reduced by ~60% in the Δ*asct*/^{RNAi}ATPϵ-F1β.i after 4 days of induction, compared with the wild-type cells (Table 3). This strongly supports the interpretation that death of the Δ*asct*/^{RNAi}ATPϵ-F1β.i mutant is due to a great reduction of the mitochondrial ATP production. A lower reduction (~30%) was observed for the Δ*asct* and ^{RNAi}ATPϵ-F1β.i single mutants, matching their moderate growth phenotypes (Figs. 1*C* and 6*C*). We conclude that the ASCT/SCoAS cycle and ATPϵ can both supply sufficient mitochondrial ATP for survival and growth. The great reduction of the intracellular amounts of ATP in the non-induced Δ*asct*/^{RNAi}ATPϵ-F1β.ni cell line (~50%) is certainly due to the reduction of the ATPϵ-F1β expression in the ASCT null background (Fig. 6*D*, *inset*). In contrast, the impact of *ACH* gene deletion on the intracellular amounts of ATP is minor (Table 3), in agreement with the absence of a growth phenotype.

DISCUSSION

The procyclic form of *T. brucei* excretes mainly acetate and succinate when glucose is metabolized (12). The enzymes involved in the glycosomal and mitochondrial succinate production have been characterized (11, 35); however, the mitochondrial metabolic pathway leading to acetate production was not completely elucidated. Unraveling the topology of the acetate branch is particularly relevant because we recently showed that acetate production in the mitochondrion of the procyclic trypanosomes is essential for *de novo* fatty acids biosynthesis (32). Indeed, trypanosomes have replaced the canonical citrate shuttle by a so-called "acetate shuttle" to transfer acetyl-CoA produced in the mitochondrion to the cytosol, where fatty acid biosynthesis is initiated (steps 1, 2, and 5 in supplemental Fig. S1). Here we show that two mitochondrial enzymatic activities (ASCT and ACH) are responsible for acetate production from acetyl-CoA. These activities are encoded by the *ASCT* gene

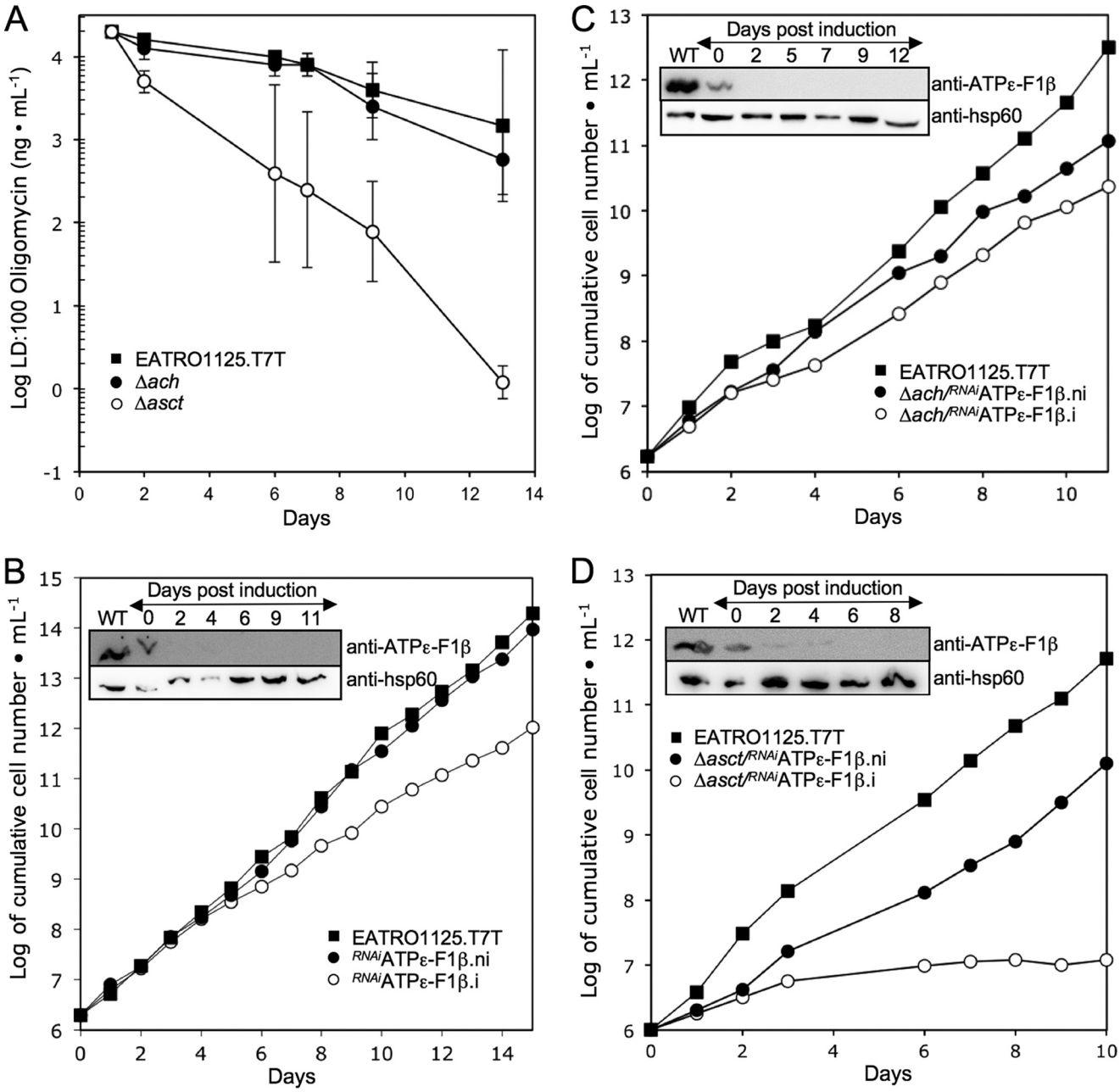

FIGURE 6. **ATP is primarily produced by the ASCT/SCoAS cycle and oxidative phosphorylation in the procyclic cells.** *A*, oligomycin sensitivity of the EATRO1125.T7T, Δ*ach*, and Δ*asct* cell lines (5×10^5 cells/ml) incubated in SDM79 medium. The drug concentration required to kill all cells (*LD:100*) is plotted over the incubation time with the drug. A logarithmic scale is used for the drug concentration, and the mean ± S.D. ($n = 3$) is presented. *B–D*, growth curves of the ^{RNAi}ATPε-F1β, Δ*ach*/^{RNAi}ATPε-F1β, and Δ*asct*/^{RNAi}ATPε-F1β cell lines incubated in the presence (*.i*; ○) or in the absence (*.ni*; ●) of tetracycline. Cells were maintained in the exponential growth phase (between 10^6 and 10^7 cells/ml) by dilution, and cumulative cell numbers are calculated. The *insets* show Western blot controls of ATPε-F1β expression in the respective cell lines upon tetracycline induction. Anti-hsp60 was used as an internal reference.

(Tb11.02.0290) (13) and the *ACH* gene (*Tb927.3.4260*), both expressed in the mitochondrion of procyclic trypanosomes. ACH activity is largely described in plants and animals, but only one ACH activity was earlier reported in a parasite, the nematode *Ascaris suum* (36). However, the gene has not yet been identified in the incomplete *A. suum* genome database (2). Trypanosomatids are the first organisms known to express two mitochondrial enzymatic activities for acetate production. Such redundancy has also been proposed for *N. gruberi*, whose genome contains *ASCT* and acetyl-CoA synthetase (ADP-forming) genes (10), yet there is no biochemical evidence.

Acetate production has also been proposed to be coupled to ATP production through the ASCT/SCoAS cycle (3, 13, 37). In glucose-rich conditions, oxidative phosphorylation is not essential for growth and ATP production in the EATRO1125 procyclic trypanosome strain, whereas substrate-level phosphorylation is essential for the parasite (14, 34, 38). The mitochondrion is involved in both oxidative phosphorylation through ATPε and substrate level phosphorylation by SCoAS. It was previously proposed that succinyl-CoA produced during acetate formation by ASCT is recycled to succinate by SCoAS, with a concomitant production of ATP (3). In agreement with

TABLE 3

Intracellular ATP concentration

ATP concentrations (nmol/mg of protein) were determined on trypanosome extracts using the firefly luciferase bioluminescence assay.

Cell lines[a]	[ATP]	Student's *t* test (compared with WT)[b]
	nmol/mg protein	
EATRO1125.T7T (WT)	3.88 ± 0.32	NA[c]
Δ*ach*	3.36 ± 0.34	0.14354[d]
Δ*asct*	2.72 ± 0.58	0.02311
^{RNAi}ATPϵ-F1β.ni	3.43 ± 1.15	0.55343[d]
^{RNAi}ATPϵ-F1β.i (4 days)	2.46 ± 0.43	0.02092[e]
Δ*asct*/^{RNAi}ATPϵ-F1β.ni	2.00 ± 0.32	0.00035
Δ*asct*/^{RNAi}ATPϵ-F1β.i (1 day)	1.84 ± 0.47	0.00081
Δ*asct*/^{RNAi}ATPϵ-F1β.i (2 days)	1.78 ± 0.35	0.00093
Δ*asct*/^{RNAi}ATPϵ-F1β.i (3 days)	1.69 ± 0.14	0.00003
Δ*asct*/^{RNAi}ATPϵ-F1β.i (4 days)	1.57 ± 0.24	0.00030[e]

[a] .i, RNAi cell lines tetracycline-induced during 1–4 days, depending on the cell line and the experiments; .ni, non-induced RNAi cell lines.
[b] Statistical significance for the difference in the ATP levels between the EATRO1125.T7T (WT) cells and the other cell lines was determined using Student's *t* test (bilateral and equal variance parameters). Statistical differences are significant for values of <0.05.
[c] NA, not applicable.
[d] Not significant.
[e] Statistical difference between the ^{RNAi}ATPϵ-F1β.i and Δ*asct*/^{RNAi}ATPϵ-F1β.i (4 days) is 0.0267.

this hypothesis, down-regulation of SCoAS expression by RNAi is lethal for the procyclic trypanosomes (37). However, SCoAS is a TCA cycle enzyme also involved in proline catabolism and may be essential for purposes other than ATP production through the ASCT/SCoAS cycle (see supplemental Fig. S1). Here, we directly demonstrate that the ASCT/SCoAS cycle is involved in ATP production and is essential for parasite viability when oxidative phosphorylation is inhibited. Interestingly, the ^{RNAi}ASCT.i and ^{RNAi}ATPϵ-F1β.i single mutants show a similar reduction of their doubling time (Figs. 1*C* and 6*B*) and of their intracellular ATP concentrations (Table 3), suggesting that the ASCT/SCoAS cycle and oxidative phosphorylation equally contribute to ATP generation and that both are required for maximal growth rate in glucose-rich medium.

In contrast, production of acetate through ACH is not coupled to ATP production because we observed neither a growth phenotype with the Δ*ach*/^{RNAi}ATPϵ-F1β double mutant nor a significant oligomycin sensitivity of the Δ*ach* single mutant. Furthermore, the recombinant ACH does not show a CoA-transferase activity to succinate. This raises questions about competition of ACH with ATP production in the acetate branch because ASCT and ACH share the same pool of substrate (mitochondrial acetyl-CoA). In procyclic extracts, the ASCT maximum velocity is at least 10-fold higher compared with ACH (58 and <5 milliunits/mg of protein, respectively) (13). This suggests that the ACH contribution to acetate production is minor in the wild type cells grown in standard glucose-rich conditions. This is consistent with acetate production in the ^{RNAi}ASCT.i and Δ*ach* mutants, which is at a level of ~70% or close to 100%, respectively (Table 1). The relatively low ACH specific activity in *T. brucei* is consistent with its low k_{cat} compared with the rat liver cytosolic ACH (2.7 *versus* 341 s^{-1}) (39). It is, however, noteworthy that its k_{cat} is similar to that of the rat liver mitochondrial 3-ketoacyl-CoA thiolase, which shows an acetyl-CoA thioesterase activity (1.2 s^{-1}) (40). Although the contribution of ACH is low in procyclic trypanosomes grown in glucose-rich conditions, ATP production in the acetate branch may be tuned by regulation of ACH or ASCT expression and/or activities in other physiological conditions. For instance, in the absence of glucose, the procyclic cells considerably increase their mitochondrial capacity for ATP production. First, the rate of proline degradation is ~6-fold increased (34), with an estimated 10-fold increase of the mitochondrial production of reducing equivalents (41). Consequently, electron flow increase through the respiratory chain may lead to an increase of ATP production by oxidative phosphorylation (14). Second, ATP production by the TCA cycle SCoAS step increases proportionately with the increase of proline consumption (~6-fold) (see supplemental Fig. S1). Third, in these glucose-depleted conditions, high amounts of acetate are nevertheless produced from threonine to feed fatty acid *de novo* biosynthesis, further adding to ATP production through the ASCT/SCoAS cycle (32, 34). ATP is exported to the cytoplasm in low glucose conditions, but ATP production has to be regulated to prevent mitochondrial ADP depletion. One way to achieve this in kinetoplastids is redirecting the electron flow toward the trypanosome alternative oxidase, which is not involved in proton gradient and hence ATP production. We propose that modulating the ACH and/or ASCT activity ratio is an alternative mechanism. It is noteworthy that the trypanosome alternative oxidase does not exist in *Leishmania* spp. (42), which may therefore rely on the *ASCT* and *ACH* pair present in the genome (TriTrypDB).

Another possible function of ACH may be to hydrolyze the CoA radical of other acyl-CoAs because ACH belongs to the acyl-CoA thioesterase family, which shows a broad substrate specificity ranging from acetyl-CoA to long-chain acyl-CoAs (43). The *T. brucei* enzyme is specific for short-chain fatty acids (C2, C4, and to a lesser extent C6) and shows no detectable activity with longer acyl-CoAs (from C8 to C20). Consequently, ACH is not directly involved in fatty acid metabolism by acyl-CoA thioesterification. Interestingly, the *T. brucei* ACH shows a particularly high specific activity for C4 acyl-CoAs (butyryl-CoA, acetoacetyl-CoA, β-hydroxybutyryl-CoA, and crotonyl-CoA), which are precursors of ketone bodies (β-hydroxybutyrate and acetoacetate). The procyclic trypanosomes produce and excrete β-hydroxybutyrate from proline metabolism (14) as well as from glucose metabolism when acetate production is reduced in the Δ*asct* and ^{RNAi}ASCT.i mutants (13) or succinate production is abolished in the Δ*pepck* mutant (16). ACH could be involved in ketone body production by hydrolyzing β-hydroxybutyryl-CoA and/or acetoacetyl-CoA into β-hydroxybutyrate and acetoacetate, respectively. The role of ketone body production from proline metabolism in wild type trypanosomes is unknown. Detailed analyses of intracellular metabolites in the Δ*ach* cell line will be helpful to understand this unexpected pathway.

In conclusion, we have demonstrated that the ASCT/SCoAS cycle is a key player in ATP production by substrate level phosphorylation in the mitochondrion of procyclic trypanosomes, and its contribution to ATP production seems equivalent to oxidative phosphorylation by the mitochondrial ATPϵ. ASCT has been described in several other parasites, where it probably also plays an important or essential role in ATP production (1, 2). These organisms are not amenable or are poorly amenable

to reverse genetic approaches, and no ASCT inhibitors are known yet, preventing functional characterization of the enzyme's role. For anaerobic or microaerophilic pathogenic parasites, ASCT may be an attractive target for inhibitor development.

Acknowledgments—We thank Dave Speijer (Amsterdam, Netherlands) for providing the immune serum against the F1β subunit of the F_0/F_1-ATP synthase, Paul P. Van Veldhoven (Leuven, Belgium) for the ACH activity protocol, and Michel Rigoulet (Bordeaux, France) for the luminometer.

REFERENCES

1. Bringaud, F., Ebikeme, C., and Boshart, M. (2010) Acetate and succinate production in amoebae, helminths, diplomonads, trichomonads, and trypanosomatids. Common and diverse metabolic strategies used by parasitic lower eukaryotes. *Parasitology* **137,** 1315–1331
2. Tielens, A. G., van Grinsven, K. W., Henze, K., van Hellemond, J. J., and Martin, W. (2010) Acetate formation in the energy metabolism of parasitic helminths and protists. *Int. J. Parasitol.* **40,** 387–397
3. Van Hellemond, J. J., Opperdoes, F. R., and Tielens, A. G. (1998) Trypanosomatidae produce acetate via a mitochondrial acetate:succinate CoA transferase. *Proc. Natl. Acad. Sci. U.S.A.* **95,** 3036–3041
4. Saz, H. J., deBruyn, B., and de Mata, Z. (1996) Acyl-CoA transferase activities in homogenates of *Fasciola hepatica* adults. *J. Parasitol.* **82,** 694–696
5. Ghedin, E., Wang, S., Spiro, D., Caler, E., Zhao, Q., Crabtree, J., Allen, J. E., Delcher, A. L., Guiliano, D. B., Miranda-Saavedra, D., Angiuoli, S. V., Creasy, T., Amedeo, P., Haas, B., El-Sayed, N. M., Wortman, J. R., Feldblyum, T., Tallon, L., Schatz, M., Shumway, M., Koo, H., Salzberg, S. L., Schobel, S., Pertea, M., Pop, M., White, O., Barton, G. J., Carlow, C. K., Crawford, M. J., Daub, J., Dimmic, M. W., Estes, C. F., Foster, J. M., Ganatra, M., Gregory, W. F., Johnson, N. M., Jin, J., Komuniecki, R., Korf, I., Kumar, S., Laney, S., Li, B. W., Li, W., Lindblom, T. H., Lustigman, S., Ma, D., Maina, C. V., Martin, D. M., McCarter, J. P., McReynolds, L., Mitreva, M., Nutman, T. B., Parkinson, J., Peregrin-Alvarez, J. M., Poole, C., Ren, Q., Saunders, L., Sluder, A. E., Smith, K., Stanke, M., Unnasch, T. R., Ware, J., Wei, A. D., Weil, G., Williams, D. J., Zhang, Y., Williams, S. A., Fraser-Liggett, C., Slatko, B., Blaxter, M. L., and Scott, A. L. (2007) Draft genome of the filarial nematode parasite *Brugia malayi*. *Science* **317,** 1756–1760
6. van Hoek, A. H., Akhmanova, A. S., Huynen, M. A., and Hackstein, J. H. (2000) A mitochondrial ancestry of the hydrogenosomes of *Nyctotherus ovalis*. *Mol. Biol. Evol.* **17,** 202–206
7. Steinbüchel, A., and Müller, M. (1986) Anaerobic pyruvate metabolism of *Tritrichomonas foetus* and *Trichomonas vaginalis* hydrogenosomes. *Mol. Biochem. Parasitol.* **20,** 57–65
8. Marvin-Sikkema, F. D., Pedro Gomes, T. M., Grivet, J. P., Gottschal, J. C., and Prins, R. A. (1993) Characterization of hydrogenosomes and their role in glucose metabolism of *Neocallimastix* sp. L2. *Arch. Microbiol.* **160,** 388–396
9. Denoeud, F., Roussel, M., Noel, B., Wawrzyniak, I., Da Silva, C., Diogon, M., Viscogliosi, E., Brochier-Armanet, C., Couloux, A., Poulain, J., Segurens, B., Anthouard, V., Texier, C., Blot, N., Poirier, P., Ng, G. C., Tan, K. S., Artiguenave, F., Jaillon, O., Aury, J. M., Delbac, F., Wincker, P., Vivarès, C. P., and El Alaoui, H. (2011) Genome sequence of the stramenopile Blastocystis, a human anaerobic parasite. *Genome Biol.* **12,** R29
10. Fritz-Laylin, L. K., Prochnik, S. E., Ginger, M. L., Dacks, J. B., Carpenter, M. L., Field, M. C., Kuo, A., Paredez, A., Chapman, J., Pham, J., Shu, S., Neupane, R., Cipriano, M., Mancuso, J., Tu, H., Salamov, A., Lindquist, E., Shapiro, H., Lucas, S., Grigoriev, I. V., Cande, W. Z., Fulton, C., Rokhsar, D. S., and Dawson, S. C. (2010) The genome of *Naegleria gruberi* illuminates early eukaryotic versatility. *Cell* **140,** 631–642
11. Besteiro, S., Biran, M., Biteau, N., Coustou, V., Baltz, T., Canioni, P., and Bringaud, F. (2002) Succinate secreted by *Trypanosoma brucei* is produced by a novel and unique glycosomal enzyme, NADH-dependent fumarate reductase. *J. Biol. Chem.* **277,** 38001–38012
12. Bringaud, F., Rivière, L., and Coustou, V. (2006) Energy metabolism of trypanosomatids. Adaptation to available carbon sources. *Mol. Biochem. Parasitol.* **149,** 1–9
13. Rivière, L., van Weelden, S. W., Glass, P., Vegh, P., Coustou, V., Biran, M., van Hellemond, J. J., Bringaud, F., Tielens, A. G., and Boshart, M. (2004) Acetyl:succinate CoA-transferase in procyclic *Trypanosoma brucei*. Gene identification and role in carbohydrate metabolism. *J. Biol. Chem.* **279,** 45337–45346
14. Coustou, V., Biran, M., Breton, M., Guegan, F., Rivière, L., Plazolles, N., Nolan, D., Barrett, M. P., Franconi, J. M., and Bringaud, F. (2008) Glucose-induced remodeling of intermediary and energy metabolism in procyclic *Trypanosoma brucei*. *J. Biol. Chem.* **283,** 16342–16354
15. Brun, R., and Schönenberger, M. (1979) Cultivation and *in vitro* cloning or procyclic culture forms of *Trypanosoma brucei* in a semidefined medium. Short communication. *Acta Trop.* **36,** 289–292
16. Ebikeme, C., Hubert, J., Biran, M., Gouspillou, G., Morand, P., Plazolles, N., Guegan, F., Diolez, P., Franconi, J. M., Portais, J. C., and Bringaud, F. (2010) Ablation of succinate production from glucose metabolism in the procyclic trypanosomes induces metabolic switches to the glycerol 3-phosphate/dihydroxyacetone phosphate shuttle and to proline metabolism. *J. Biol. Chem.* **285,** 32312–32324
17. Bringaud, F., Robinson, D. R., Barradeau, S., Biteau, N., Baltz, D., and Baltz, T. (2000) Characterization and disruption of a new *Trypanosoma brucei* repetitive flagellum protein, using double-stranded RNA inhibition. *Mol. Biochem. Parasitol.* **111,** 283–297
18. Bringaud, F., Baltz, D., and Baltz, T. (1998) Functional and molecular characterization of a glycosomal PP_i-dependent enzyme in trypanosomatids. Pyruvate, phosphate dikinase. *Proc. Natl. Acad. Sci. U.S.A.* **95,** 7963–7968
19. Ngô, H., Tschudi, C., Gull, K., and Ullu, E. (1998) Double-stranded RNA induces mRNA degradation in *Trypanosoma brucei*. *Proc. Natl. Acad. Sci. U.S.A.* **95,** 14687–14692
20. Wirtz, E., Leal, S., Ochatt, C., and Cross, G. A. (1999) A tightly regulated inducible expression system for conditional gene knock-outs and dominant-negative genetics in *Trypanosoma brucei*. *Mol. Biochem. Parasitol.* **99,** 89–101
21. Harlow, E., and Lane, D. (eds). (1988) *Antibodies: A Laboratory Manual*, Cold Spring Harbor Laboratory, Cold Spring Harbor, NY
22. Sambrook, J., Fritsch, E. F., and Maniatis, T. (eds) (1989) *Molecular Cloning: A Laboratory Manual*, Cold Spring Harbor Laboratory, Cold Spring Harbor, NY
23. Speijer, D., Breek, C. K., Muijsers, A. O., Hartog, A. F., Berden, J. A., Albracht, S. P., Samyn, B., Van Beeumen, J., and Benne, R. (1997) Characterization of the respiratory chain from cultured *Crithidia fasciculata*. *Mol. Biochem. Parasitol.* **85,** 171–186
24. Bringaud, F., Peyruchaud, S., Baltz, D., Giroud, C., Simpson, L., and Baltz, T. (1995) Molecular characterization of the mitochondrial heat shock protein 60 gene from *Trypanosoma brucei*. *Mol. Biochem. Parasitol.* **74,** 119–123
25. Choe, J., Guerra, D., Michels, P. A., and Hol, W. G. (2003) *Leishmania mexicana* glycerol-3-phosphate dehydrogenase showed conformational changes upon binding a bi-substrate adduct. *J. Mol. Biol.* **329,** 335–349
26. Ramsay, R. R., and Tubbs, P. K. (1975) The mechanism of fatty acid uptake by heart mitochondria. An acylcarnitine-carnitine exchange. *FEBS Lett.* **54,** 21–25
27. Mannaerts, G. P., Debeer, L. J., Thomas, J., and De Schepper, P. J. (1979) Mitochondrial and peroxisomal fatty acid oxidation in liver homogenates and isolated hepatocytes from control and clofibrate-treated rats. *J. Biol. Chem.* **254,** 4585–4595
28. Coustou, V., Biran, M., Besteiro, S., Rivière, L., Baltz, T., Franconi, J. M., and Bringaud, F. (2006) Fumarate is an essential intermediary metabolite produced by the procyclic *Trypanosoma brucei*. *J. Biol. Chem.* **281,** 26832–26846
29. Akoka, S., Barantin, L., and Trierweiler, M. (1999) Concentration measurement by proton NMR using the ERETIC method. *Anal. Chem.* **71,** 2554–2557
30. Heape, A. M., Juguelin, H., Boiron, F., and Cassagne, C. (1985) Improved one-dimensional thin layer chromatographic technique for polar lipids.

J. Chromatogr. **322,** 391–395
31. Lemasters, J. J., and Hackenbrock, C. R. (1979) Continuous measurement of adenosine triphosphate with firefly luciferase luminescence. *Methods Enzymol.* **56,** 530–544
32. Riviere, L., Moreau, P., Allmann, S., Hahn, M., Biran, M., Plazolles, N., Franconi, J. M., Boshart, M., and Bringaud, F. (2009) *Proc. Natl. Acad. Sci. U.S.A.* **106,** 12694–12699
33. Spitznagel, D., Ebikeme, C., Biran, M., Nic a' Bháird, N., Bringaud, F., Henehan, G. T., and Nolan, D. P. (2009) Alanine aminotransferase of Trypanosoma brucei–a key role in proline metabolism in procyclic life forms. *FEBS J.* **276,** 7187–7199
34. Lamour, N., Rivière, L., Coustou, V., Coombs, G. H., Barrett, M. P., and Bringaud, F. (2005) Proline metabolism in procyclic *Trypanosoma brucei* is down-regulated in the presence of glucose. *J. Biol. Chem.* **280,** 11902–11910
35. Coustou, V., Besteiro, S., Rivière, L., Biran, M., Biteau, N., Franconi, J. M., Boshart, M., Baltz, T., and Bringaud, F. (2005) A mitochondrial NADH-dependent fumarate reductase involved in the production of succinate excreted by procyclic *Trypanosoma brucei*. *J. Biol. Chem.* **280,** 16559–16570
36. de Mata, Z. S., deBruyn, B., and Saz, H. J. (1997) Acetyl-CoA hydrolase activity and function in *Ascaris suum* muscle mitochondria. *Comp. Biochem. Physiol. B Biochem. Mol. Biol.* **116,** 379–383
37. Bochud-Allemann, N., and Schneider, A. (2002) Mitochondrial substrate level phosphorylation is essential for growth of procyclic *Trypanosoma brucei*. *J. Biol. Chem.* **277,** 32849–32854
38. Coustou, V., Besteiro, S., Biran, M., Diolez, P., Bouchaud, V., Voisin, P., Michels, P. A., Canioni, P., Baltz, T., and Bringaud, F. (2003) ATP generation in the *Trypanosoma brucei* procyclic form. Cytosolic substrate level is essential, but not oxidative phosphorylation. *J. Biol. Chem.* **278,** 49625–49635
39. Suematsu, N., Okamoto, K., and Isohashi, F. (2003) Simple and unique purification by size-exclusion chromatography for an oligomeric enzyme, rat liver cytosolic acetyl-coenzyme A hydrolase. *J. Chromatogr. B Analyt. Technol. Biomed. Life Sci.* **790,** 239–244
40. Yamashita, H., Itsuki, A., Kimoto, M., Hiemori, M., and Tsuji, H. (2006) Acetate generation in rat liver mitochondria. Acetyl-CoA hydrolase activity is demonstrated by 3-ketoacyl-CoA thiolase. *Biochim. Biophys. Acta* **1761,** 17–23
41. Bringaud, F., Barrett, M. P., and Zilberstein, D. (2012) Multiple roles of proline transport and metabolism in trypanosomatids. *Front. Biosci.* **17,** 349–374
42. Chaudhuri, M., Ott, R. D., and Hill, G. C. (2006) Trypanosome alternative oxidase. From molecule to function. *Trends Parasitol.* **22,** 484–491
43. Hunt, M. C., and Alexson, S. E. (2002) The role Acyl-CoA thioesterases play in mediating intracellular lipid metabolism. *Prog. Lipid. Res.* **41,** 99–130

ATP Synthesis-coupled and -uncoupled Acetate Production from Acetyl-CoA by Mitochondrial Acetate:Succinate CoA-transferase and Acetyl-CoA Thioesterase in *Trypanosoma*

Yoann Millerioux, Pauline Morand, Marc Biran, Muriel Mazet, Patrick Moreau, Marion Wargnies, Charles Ebikeme, Kamel Deramchia, Lara Gales, Jean-Charles Portais, Michael Boshart, Jean-Michel Franconi and Frédéric Bringaud

J. Biol. Chem. 2012, 287:17186-17197.
doi: 10.1074/jbc.M112.355404 originally published online April 2, 2012
